

The door to Dor: Tracing unseen anthropogenic impact in an ancient port

Michael Lazar¹  | Uri Basson^{1,2} | Ashley G. Himmelstein³ | Thomas E. Levy^{4,5} | Ehud Arkin Shalev³  | Assaf Yasur-Landau^{3,6} 

¹Dr. Moses Strauss Department of Marine Geosciences, Charney School of Marine Sciences, University of Haifa, Haifa, Israel

²GeoSense Ltd., Netanya, Israel

³Department of Maritime Civilizations, Charney School of Marine Sciences, University of Haifa, Haifa, Israel

⁴Department of Anthropology, University of California, San Diego, California, USA

⁵Levant and Cyber-Archaeology Laboratory, Scripps Center for Marine Archaeology, University of California, San Diego, California, USA

⁶The Recanati Institute for Maritime Studies (RIMS), University of Haifa, Haifa, Israel

Correspondence

Michael Lazar, Dr. Moses Strauss Department of Marine Geosciences, Charney School of Marine Sciences, University of Haifa, Haifa 3498838, Israel.

Email: mlazar@univ.haifa.ac.il

Scientific editing by Patrick Nunn.

Funding information

Israel Science Foundation, Grant/Award Number: 495/18

Abstract

An on-land frequency domain electromagnetic geophysical survey was conducted across a tombolo delimiting the southern bay of Tel Dor (northern Israel) to the south. It was accompanied by a marine archaeological survey adjacent to its northern edge. Results indicate a deep channel connecting the bay and the Tantura Lagoon to the south. At its northern exit, an NW–SE trending square anomaly is visible in the geophysical data, buried underneath centuries of sand accumulation. It is parallel and similar in shape and scale to a Hellenistic feature observed in satellite data and excavated during the underwater archaeological survey. It seems that during the beginning/Middle Bronze Age, a natural or manmade channel was utilized as an entrance to the bay. As sea levels rose and sand began to accumulate, the channel was periodically filled in and would have needed to have been cleared. Eventually, it became too expensive or inconvenient to maintain, probably during the Byzantine period. The southern anchorage was abandoned for more favorable conditions to the north of the Tel. The sequence of events shows how ancient builders first utilized a natural channel, maintained it as sea levels rose, and abandoned it when it became too problematic to maintain.

KEYWORDS

ancient port, anthropogenic impact, archaeology, frequency domain electromagnetics, sea-level rise

1 | GENERAL INTRODUCTION

Tel Dor located on the Carmel Coast, 21 km south of present-day Haifa and 13 km north of Caesarea (Figure 1), was settled in the Middle and Late Bronze Ages, during most of the Iron Age, and from the Persian period to at least the Late Roman and Byzantine periods (Gilboa & Sharon, 2008; Nitschke et al., 2011; Raban, 1995; Stern, 1994). It is located on an eolianite ridge, separated from the nearby Mt. Carmel by a narrow alluvial area. This would have provided the settlement with a minimal agricultural hinterland, thus necessitating maritime connectivity and trade. Three bays are located adjacent to the site (Figure 1b). From north to south, these are the North Bay,

the Love Bay, and the South Bay, the latter located immediately south of the Tel that comprises Dor. The Tantura Lagoon, in which more than 20 shipwrecks of the Roman–Ottoman period were found, is located south of the South Bay and separated from it by a large tombolo (Kahanov, 2011; Raban, 1995). While there is ample evidence for maritime activity and related structures in the northern part of the South Bay immediately south of the Tel (Section 2.2; ArkinShalev et al., 2019a, 2019b), there is, to date, a little information on any structures near the area of the tombolo. Raban (1995) theorized that a now buried passage existed between the South Bay and the Tantura Lagoon, which lies to the south. According to the author, at its time of use as an anchorage, the western approach to

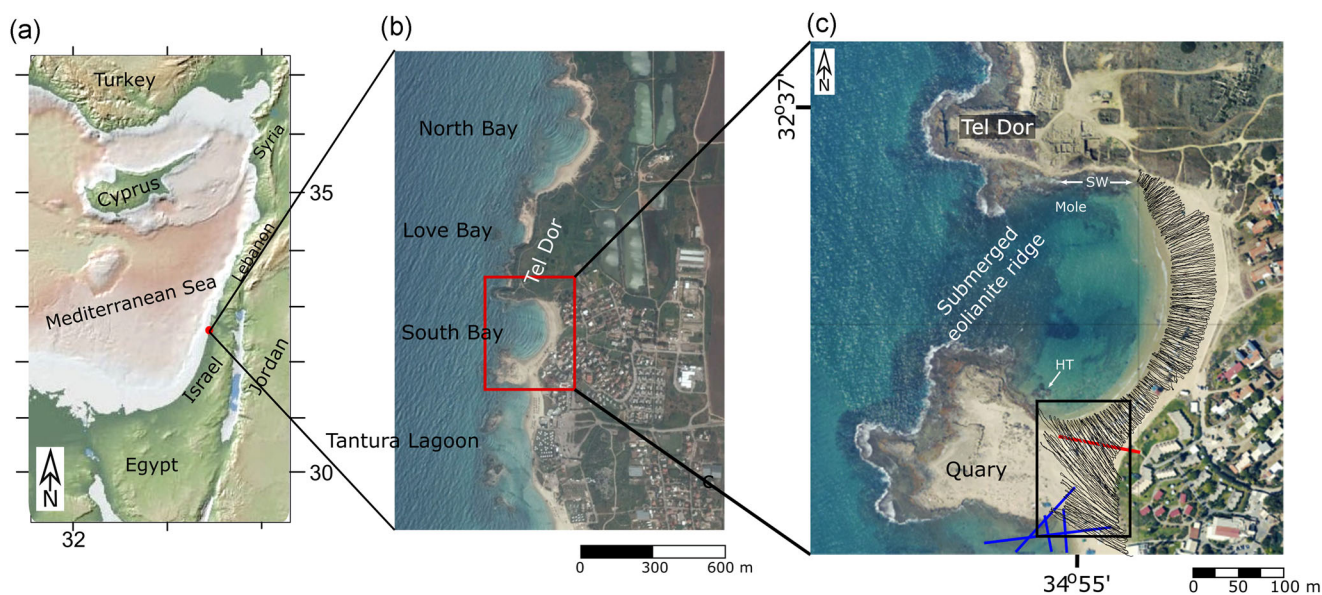


FIGURE 1 Location maps (a) the location of Tel Dor along the Israeli coast (b) satellite image showing the two South Bay, which is the focus of this study, and the location of the other bays lying to the north and south (c) the South Bay of Dor. Red line represents the approximate location of the refraction line shown in Figure 4. Blue lines are from the study of Swarzenski et al. (2006). Thin black lines show the exact path walked during the FDEM survey used in this study and the black rectangle marks the location of the tombolo—the main focus of this study. SW—massive Iron Age 1b sea wall. FDEM, frequency domain electromagnetic; HT, Hellenistic Tower [Color figure can be viewed at wileyonlinelibrary.com]

the bay would have been almost totally blocked to the water level by a now underwater eolianite ridge.

This article uses a combination of geophysical and archaeological methods to explore the idea of such a passage and accompanying structures. As such, it sheds light on the interactions between anthropogenic activities and natural processes such as sea-level rise in the ancient world.

2 | ENVIRONMENTAL AND ARCHAEOLOGICAL CONTEXT

2.1 | The environment of the South Bay of Dor

Sivan et al. (2004) provided information on the geomorphology and development of Dor's South Bay, especially with respect to the sand cover. Seismic refraction profiles were examined in conjunction with a series of cores that were analyzed for sedimentary properties and for correlation. The authors deduced the thickness of the sand, clay, and bedrock cover from their data. Only one borehole (Core #4) and one seismic refraction line (Line #4) fall within the current study area, although neither appears in the above-mentioned publication. Therefore, the original report from the Geophysical Institute of Israel was used (Beck & Kravtsov, 1998 [available upon request]). The refraction line (see Figure 1c for location) will be referred to in Section 5. Since the exact location of the borehole could not be determined, it was not used in this study.

The South Bay of Dor is characterized by a 5-m sand cover that lies above an additional 5 m of clay. At the base of the clay layer,

eolianite bedrock can be found (Sivan et al., 2004). The deposition of the top clay occurred in a wetland/coastal marsh setting and was dated to 8938–8166 BC (corrected calibrated ^{14}C by Lazar et al., 2018). In the Tantura Lagoon (Figure 1), the onset of sand accumulation was dated to 5100 ± 500 cal YBP by Kadosh et al. (2004) by infrared stimulated luminescence. This was corrected for anomalous fading to 6200 ± 700 cal YBP by Lazar et al. (2018). Regardless, as Mediterranean Sea levels rose to 1–2 m below their present-day level, sand began to reach and accumulate along the coast (Cohen-Seffer et al., 2005; Sivan et al., 2004), probably due to a combination of longshore and eolian transport.

A time-series resistivity survey was conducted by Swarzenski et al. (2006) to assess groundwater discharge adjacent to the tombolo (Figure 1c). Since the focus of their study was on the deeper subsurface, the resolution of their data in the top few meters is relatively poor. However, the presence of a saturated sand layer (as opposed to eolianite or silt/clay) can be inferred from their results, extending from the surface down to a depth of about 5–6 m across the tombolo. Another important finding from their study was the fact that groundwater is actively seeping to the surface in the area of the tombolo.

2.2 | Maritime activity and related structures in the South Bay of Dor

Excavations of Tel Dor began in 1924 and have continued intermittently until today. There is archaeological and historical evidence of maritime activities in the bays of Dor, which date to as early as the

Middle and Late Bronze Age through the Iron Age and well into the Byzantine period (ArkinShalev et al., 2019a). The Wen-Amon text refers to an 11th century BCE harbor at Dor, out of which a large fleet of ships operated (Gilboa, 2015; Yasur-Landau, 2019). The South Bay, adjacent to the Tel, was no doubt used for anchoring in the Bronze and Iron Ages, as indicated by underwater surveys that documented numerous stone anchors and pottery (Kingsley & Raveh, 1996; Lazar et al., 2018). Two massive parallel ashlar walls, semi-submerged by the waterline at the northern edge of the South Bay (Figure 1c), were previously interpreted as quays belonging to the Late Bronze Age and to the Sea People harbor of Dor (Raban, 1995). Recent excavations and pottery associated with these walls demonstrated that these features belonged to a massive Iron Ib coastal sea wall. During the same excavations, a massive mole made of ashlar stones (Figure 1c) dated by pottery to the Iron II period, now partially covered with a crust of biogenic rock, was found to the south of this fortification line, enabling the unloading of goods to the city (ArkinShalev et al., 2019b). Surprisingly, no remains of Hellenistic maritime infrastructure were found at Dor to date, despite the prosperity of the city and the construction of an elaborate system of fortifications in the 3rd century BCE (Sharon, 1995; Stern, 1994). Furthermore, these fortifications encircle the Tel from the east only, while the west and especially the southern part of the Tel, overlooking the South Bay, were seemingly left unprotected. During the Roman period, maritime activity moved mainly to the North Bay and the Tantura Lagoon (ArkinShalev et al., 2019a).

The aim of this study was to extend the research carried out by Lazar et al. (2018) to the south and to possibly locate additional buried structures. Special attention was paid to the area east of the ancient eolianite quarry (the “tombolo”) with the intent of testing the hypothesis that a connection existed between the South Bay and the Tantura Lagoon.

3 | METHODS

High-resolution shallow geophysical methods have become a standard in archaeological studies since they provide a noninvasive way of imaging the subsurface before a dig. The choice of the frequency domain electromagnetic (FDEM) technique was based on its proven ability to overcome obstacles like salinity and moisture (e.g. Lazar et al., 2018) that affect more conventional methods used in archaeology and neotectonics, such as ground-penetrating radar (e.g. Basson & Ginzburg, 2009; Basson et al., 2002; Bristow & Jol, 2003; Conyers, 2004; Rogers et al., 2012). The ease of use and quick scanning capability means that large areas can be covered in a relatively short time. There are no electrodes or loops to set up. Since it measures swaths, there is a little interpolation between measurements.

The FDEM method involves generating an alternating magnetic field at the transmitter. This induces an electrical eddy current in the earth, which causes a secondary magnetic field to be formed in the subsurface. This field is mainly proportional to the conductivity of the target and the frequency of the alternating field. The sensor measures quadrature

(Q , the component of the secondary field that is out of phase with respect to the primary field) and in-phase (I , the component of the secondary field that is in phase with respect to the primary field). Since the system is multifrequency, it enables measuring in several (n) frequencies simultaneously, thus measuring $Q_1... Q_n$ and $I_1... I_n$. Data can be transformed into apparent electrical conductivity (EC_a) and apparent magnetic susceptibility (MS_a), respectively, to deduce subsurface properties (Huang & Won, 2003; Huang, 2005). EC_a is a function of the coil spacing within the instrument and is thus sensor specific. Since this is constant for a given instrument, it will be referred to here simply as EC. Contrasts in EC are interpreted as differences in subsurface clay content, mineralogy, moisture, etc. (Sudduth et al., 2005, references therein). In general, as salinity increases, there is an increase in conductivity and a decrease in resistivity.

The depth of investigation can be defined as the maximum depth, for which a half-space subsurface can be detected by the FDEM system at a particular frequency. The frequency at which the electromagnetic response of a subsurface target or inhomogeneity can first be measured is determined mainly by its depth and the electromagnetic properties of the overlying layers. It is relatively independent of the type of source or receiver and the distance between them. The depth of investigation depends on the physical subsurface properties and is mainly a function of the skin depth (Huang, 2005; Spies, 1989). The skin depth δ is a function of the angular frequency of the plane wave ω , the electrical conductivity σ , and magnetic permeability μ , of the medium according to the following:

$$\delta = \sqrt{\frac{2}{\sigma\mu\omega}} \quad (1)$$

However, the practical depth of penetration is clearly empirical. According to Spies (1989), Goldshleger and Basson (2016), Goldshleger et al. (2018) and Goldshleger et al. (2019), the practical/effective depth of penetration D is

$$D \approx 1.5 \delta = 750 \left(\frac{1}{\sigma f} \right) \quad (2)$$

where f is the frequency of the wave transmitted by the FDEM system.

Simultaneous transmission of a number of frequencies means that data is obtained from different depths since lower frequencies penetrate deeper into the subsurface than the higher ones (Equation 2). Therefore, the result of the imaging is a series of frequency/depth-range maps corresponding to the integration of all subsurface data in a specific sampled volume (i.e., down to the frequency-related depths where $F_n = D_n$, Figure 2; Table 1).

A multifrequency FDEM survey was carried out from the southern edge of Tel Dor to south of Tombolo (Figure 1) using a Geophex GEM-2 sensor with a scanning depth down to 10 m and the ability to simultaneously transmit and record 10 frequencies between 25 Hz and 93 kHz (e.g., Huang & Won, 2003; Won et al., 1996). Five frequencies were selected based on lithology described by Sivan et al. (2004), the results of Lazar et al. (2018) and noise reduction analysis. These frequencies

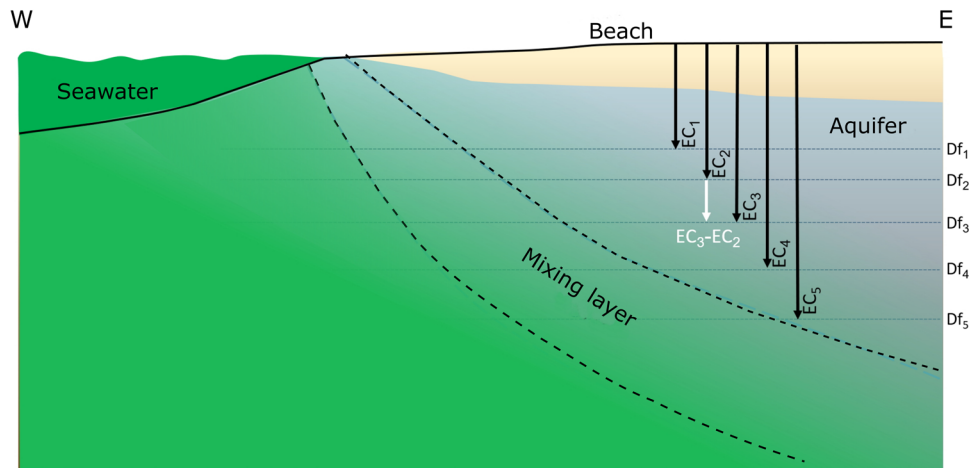


FIGURE 2 Simplified conceptual model of the study area used for inversion modeling. EC_1 – EC_5 represent the integration of all electrical conductivities down to the depths of Df_1 – Df_5 respectively (i.e., the data presented in Figure 3). EC_3 – EC_2 is an example of the “layer” for which EC is obtained by the inversion model between EC_3 and EC_2 (i.e., the data presented in Figure 4). EC, electrical conductivity; FDEM, frequency domain electromagnetic [Color figure can be viewed at wileyonlinelibrary.com]

correspond to the effective penetration depths listed in Table 1, which were calculated based on Equation 2. The distance between the source and receiver (sensor length) is 1.7 m. The survey was continuous and carried out without stopping to insure similar conditions for all lines. The sensor was carried at a height of 1 m above the surface, which corresponds to an average surface swath width of about 1 m. This increases with depth. Line spacing was monitored using a differential GPS and varied according to terrain and obstacles in the field. The average line spacing was 2 m (Figure 1c). The electrical network frequency in Israel is 50 Hz. Therefore, to avoid harmonics, the FDEM system transmitted and measured all frequencies at a rate of 25 Hz. The GEM-2 was programmed to transmit at a rate of 25 soundings per second. Data were collected by walking with the instrument at a slow speed of around 1 km/h (3.6 m/s). This resulted in an average spatial sampling of about seven measurements per meter.

Data were filtered using a nonlinear filter to remove spikes and random/ambient noise. A spatial bandpass filter was applied for antialiasing. A normalized weighted algorithm based on the half-space model was computed to create an inversion of the frequency interval for every two consecutive frequency pairs. The result is a series of EC maps that contain the integration of all electrical

conductivity of a specific depth range between a given frequency pair (Figure 2). The exact algorithm used is the proprietorship of GeoSense Ltd. This allowed for the observation of anomalies associated with subsurface geology or archaeology.

4 | RESULTS

4.1 | Geophysical survey

The results of the survey were first plotted with minimal processing since these represent the actual data collected in the field. The five EC maps are similar in their overall appearance (Figure 3). EC values on the western edge of the data from the tombolo are similar to those on the eastern, with dark blue representing values near or around 5 mS/m. Since on the western side, these values correspond to eolianite that is exposed on the surface, it can be assumed that the eastern side contains buried eolianite beneath a thin cover of sand since eolianite is not visible on the surface. This is supported by the interpretation of the refraction profile (see below). Between the two areas of extremely low values, EC increases to values between 142 and 2300 mS/m (depending on depth of penetration) indicating an absolute change in subsurface properties. This picture is consistent throughout all frequencies (i.e., depths) investigated in this study (Table 1) and we interpret this change here as a sharp transition from hard eolianite sandstone to a soft sand-filled trench or channel. While dry sand is less conductive than dry sandstone (Best, 2015 and references therein), it is also more porous, and therefore, more hydraulically conductive (Todd & Mays, 2004) Since it can be assumed with some degree of certainty that the entire area between the quarry and the beach is saturated with seawater, this would mean that wet sand should have a higher EC than wet sandstone. It is important to note that each map contains all data from the previous

TABLE 1 Transmission frequency used in this study and effective penetration depth. Values were obtained from Equations 1 and 2

Frequency (Hz)	Effective penetration (m)
2025	0–6.5
4725	0–5.3
11,025	0–4.2
25,725	0–3.2
60,025	0–2.5

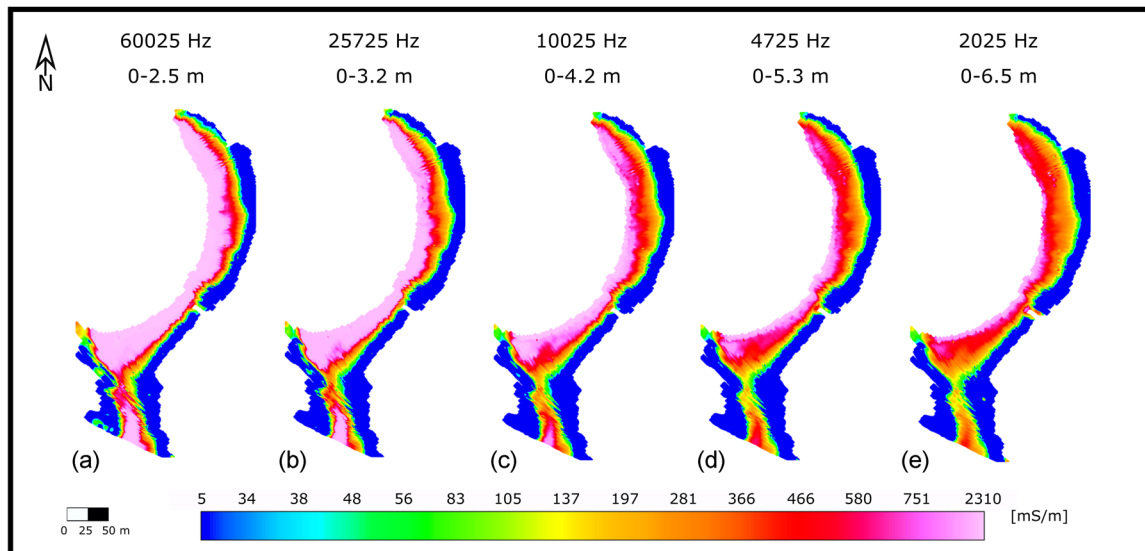


FIGURE 3 Results of the electrical conductivity (EC) obtained from the frequency domain electromagnetic (FDEM) survey with minimal processing. Units are in mS/m [Color figure can be viewed at wileyonlinelibrary.com]

depth-range, and therefore, subtle changes in EC that occur at depth are lost. To overcome this situation, simple inversion as explained above was applied.

All four inversion maps produced in this study are presented in Figure 4. The first three maps (Figures 4a-c) show a clear prominent channel cutting through the tombolo from south to north. Its width is constant with depth and is approximately 20 m wide at its narrowest. As frequencies decrease (i.e., depth increases), EC values from the assumed channel are more or less consistent (around 1750 mS/m) indicating similar fill with slightly changing properties probably due to differences in salinity. In the final depth range (5.3–6.5 m), EC values

reach their highest in the center of the channel (1775–1800 mS/m; Figure 4d, red-pink hues), which is indicative of eolianite in the analysis presented here. This would seem to imply that the assumed channel is obstructed at these depths by eolianite blocks.

Examination of the refraction profile that crosses the northern part of the tombolo (Figure 5) indicates that there are three seismic layers in the shallow subsurface that are discerned by differences in seismic velocity. The bottom-most layer (velocity of 2240 m/s) is representative of eolianite rock found in the area. According to the profile, it forms approximately 2.5 m high ridge that drops sharply to the west (across the tombolo) to around -9 m, indicating that a deep channel does in fact exist

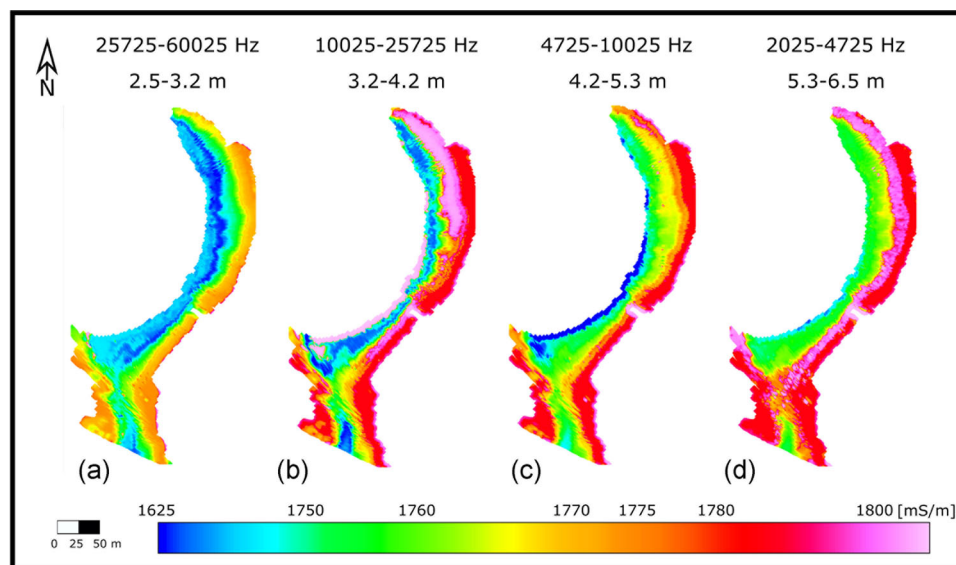


FIGURE 4 Results of the inversion modeling of the interval for every two consecutive frequency pairs. The maps present the integration of all electrical conductivity of a specific depth range between a given frequency pair [Color figure can be viewed at wileyonlinelibrary.com]

FIGURE 5 (a) electrical conductivity (EC) inversion map of the tombolo for the frequency range of 2025–4725 Hz (representing the depth slice from 5.3 to 6.5 m). Black line marks the approximate location of the refraction profile shown in (b) after Beck and Kravtsov (1998). See text for explanation. [Color figure can be viewed at wileyonlinelibrary.com]

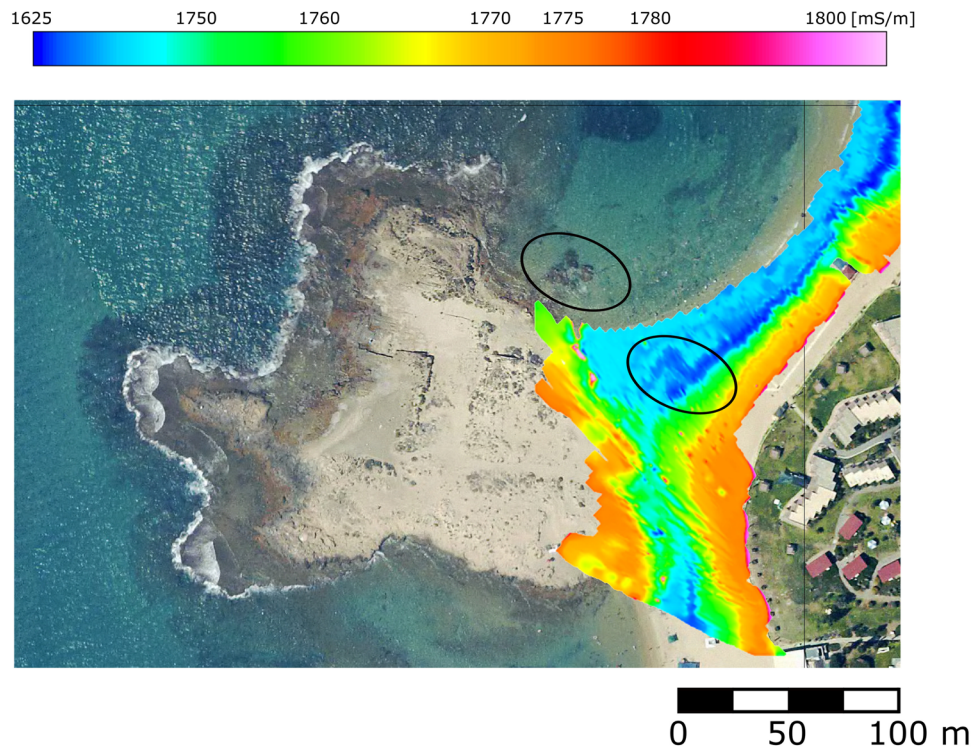
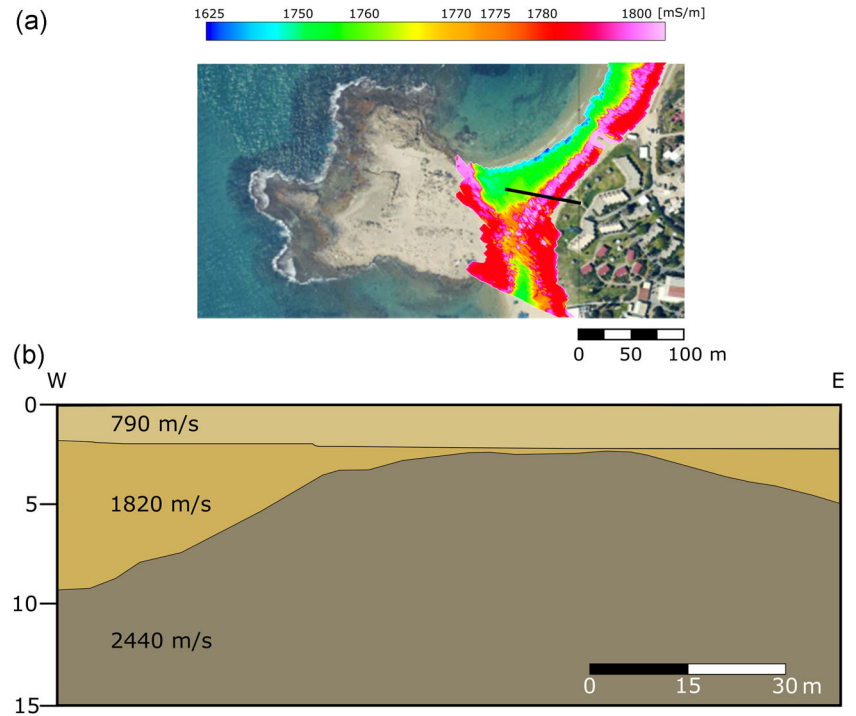


FIGURE 6 Electrical conductivity (EC) inversion map of the tombolo for the frequency range of 25,725–60,025 Hz (representing the depth slice from 2.5 to 3.2 m), superimposed on an orthophoto of the South Bay. The square anomaly visible in the FDEM image on land is marked by a black oval. Please note the submerged ashlar structure visible on the orthophoto image located in the water adjacent to the northern edge of the tombolo (also circled). [Color figure can be viewed at wileyonlinelibrary.com]

from the south to the north across the tombolo. Its infill is composed of two additional layers with seismic velocities of 1820 and 790 m/s for the central and top-most layer accordingly. While the top layer (0-ca 2 m) represents dry sand, the middle value could represent either wet sand or shales/clays (Bourbie et al., 1987). The latter could perhaps represent the clay unit dated by Sivan et al. (2004), which would then indicate an ancient infill of a natural channel. A series of cores were recently drilled along the western flank of the tombolo. The most relevant core from the southern edge indicates that there is at least 4 m of sand (G. Shteinberg [personal communication, April 12, 2019]). Therefore, we interpret the second layer as wet sand rather than shale or clay.

A comparison of the refraction profile with the deepest inversion profile (Figure 5) shows that the eolianite channel reaches depths of almost 10 m in the area just outside the northern exit of the channel. This is deeper than the deepest depth penetrated by the FDEM and therefore, does not show up on it. The refraction profile also clearly indicates there is in fact an eolianite ridge buried under a shallow cover of sand to the east of the channel as inferred above.

In addition to the channel, the FDEM data shows another prominent anomaly adjacent to the northern edge of the channel, which is currently buried under the sand. Although present to some degree on all inversion and most EC maps, it can best be seen in Figure 4a, where it appears as a clear, narrow feature of low EC values (dark blue hues, which reach values of 1630 mS/m in this area) with a conspicuous 90° angle. This is the same shape, size and follows the same orientation as the remains of an underwater building, which can be seen adjacent to the northern edge of the tombolo in satellite and orthophoto images, to be discussed below (Figure 6). These likely represent the remains of fortification, perhaps towers protecting the entrance to the bay.

4.2 | Archaeological finds

Recent underwater archaeological surveys, as well as excavations conducted by the Recanati Institute for Maritime Studies, University of Haifa, and the Scripps Center for Marine Archaeology, UC San Diego, indicate that coastal (and perhaps maritime) structures were not limited to the north edge of the South Bay. Figure 6 shows an orthophoto image where a small, square-shaped feature is clearly seen in the shallow water adjacent to the northern face of the tombolo (see also Figure 1c). It trends NE-SW and is comparable in both size and directionality to an anomaly seen in the results of the geophysical survey. An archaeological survey conducted in 2017 showed that this feature is likely a structure made of large ashlar stones. Following this discovery, an underwater excavation in 2019 to the east and to the north of this structure indicates that is a part of a much larger artificial feature with a NE-SW orientation. To date two courses of stones were found, the top one at a depth of 1.2–1.5 m below mean sea level. It is built of ashlar stones in two size groups, the larger are 1.45–1.50 m in length and 0.4–0.5 m in width, while the smaller are 0.95–1.0 m in length and 0.4 m in width. While work on the excavation still continues, some indications of the period of the construction may be ascertained. The technique

used to construct the building belongs to the Hellenistic period, and more precisely to the 3rd century BCE. The combined use of two size groups of ashlar stones, large and small, as well as the use of dry masonry, is very similar to the construction of the Hellenistic fortifications on Tel Dor itself, just north of the South Bay and especially to the Hellenistic towers in areas A and C dated to the 3rd century BCE (Sharon, 1995). The use of ashlar combined with dry masonry in a marine context using somewhat smaller stones can be seen in the Hellenistic quay and ship shed of Akko, which also belong to the 3rd century BCE (Sharvit et al., 2013). Large ashlars (but not the combination of large and small ashlars) were used in the construction of the Late Iron Age moles and quays found underwater in Atlit, some 10 km to the north of Dor (Haggi & Artzy, 2007; Yasur-Landau et al., 2018).

The stones used near the tombolo are considerably smaller than those used in the Iron Ib coastal fortifications in the northern part of the South Bay (ArkinShalev et al., 2019b). The few pottery sherds found embedded in the structure include a Hellenistic handle of a basket and a handle of an amphora. Lack of Iron Age pottery further strengthens the identification of the structure as postdating the Iron Age. At the same time, the Dor underwater structure is of pre-Roman construction since the stones are not bonded in a mortar of concrete. Concrete was first used in the area for harbor construction in the Herodian port of Caesarea (Yasur-Landau et al., 2018).

5 | DISCUSSION

The combined geophysical and archaeological data strongly suggests a southwestern entrance to the South Bay of Dor, which is comprised of a sailing channel, 20 m wide flanked from the two sides by artificial structures, perhaps towers or other elements of fortification. However, questions remain as to why such a channel would have been needed given that the bay is open to the west, which would allow a clear approach from this direction. While there is a submerged reef blocking the entrance to the bay (currently located at a water depth of 2.5–4 m in its center, which shallows to the sides), during the Bronze and Iron Ages, sea level would have been at 3–1.5 m below the present-day level, and at least 1 m below sea level in the Hellenistic period (Benjamin et al., 2017; Sivan et al., 2001). This would mean that the reef would have been under 1.5–3 m of water, which would have perhaps allowed small boats to enter from the west, but endangered larger ships. In addition, the prevailing (storm) wind direction along the coast of Israel is from the southwest (e.g., Goldsmith et al., 1990; Saaroni et al., 1998) making the approach from the west dangerous and tricky at best during times of strong winds, especially in an area with many exposed and underwater reefs. Thus, we speculate that a combined approach—allowing entrance from both the west and the south, would be appealing. If comparing to modern anchorages along the Israel coast—none are open to the sea and entrance is always from a jetty facing northwards. This is to avoid the buildup of sand within the anchorage from northward-trending longshore sediment transport (Zviely et al., 2007). However, at the time in question, this would not have been a problem due to the fact that sand had just begun to accumulate along the coast.

The dimensions of the trench (width of ~20 m at its narrowest and a depth of at least 5–6 m) indicate that it would have been wide enough and deep enough to act as a navigation channel and allow the passage of boats from the Tantara Lagoon northwards into the bay. This is strengthened by the contrast between the jagged, western border of the channel and the relatively smooth and straight eastern border (Figures 3 and 4), which forms an almost 90° angle with the straight northeastern trending ridge as it enters the bay. This would seem to indicate that the eastern eolianite ridge was cut, smoothed, and maintained possibly due to the fact that the prevailing wind direction (from the SW) would push any vessel entering the bay from the south, through the channel and toward its eastern flanks. It is possible that this flank was smoothed to minimize dangers to approaching ships.

Two possibilities exist for the formation of the channel. The first is that it was a naturally occurring phenomenon that was utilized and maintained at least until the southern bay was abandoned sometime during the Byzantine period or slightly after (ArkinShalev et al., 2019a). The accumulation of sand along the Israeli coast is thought to have begun sometime around 6900–5500 cal YBP (Lazar et al., 2018). This means that the ancient eolianite quarry to the west of the tombolo would have been an isolated island (similar to the islands found just to the south of the bay in the Tantara Lagoon; Figure 1b) at the beginning/middle of the Bronze Age when the bay was no doubt used as an anchorage (e.g., Kingsley & Raveh, 1996). As sand began to accumulate along the coast, the area between the island in the west and the newly forming coast in the east (i.e., the channel) would have been progressively filled in. The passage would have had to have been maintained and perhaps modified during the late Bronze Age or the Iron Age Ib or II when other maritime features were constructed in the South Bay.

The second possibility is that the channel is an artificial feature that could have been fabricated when eolianite was being quarried from the eolianite outcrop to be used for construction on Tel Dor. This possibility cannot be ruled out from the FDEM data as both sides of the channel exhibit similar electromagnetic signals (Figures 3 and 4). In any case, it is clear that a channel did exist between the Tantara Lagoon and the southern bay, which would have needed artificial intervention as sand began to accumulate.

The combination of sailing channels accompanied by fortifications, perhaps towers, protecting an entrance similar to that found in this study at Dor can be found in several ports in the Aegean area. In the artificial harbor at Phalasarna in Crete built in the 4th century BCE, a 120-m-long channel connected it to the sea. The channel was originally a natural underwater opening in the rock, which was then widened to between 10 and 12 m. The harbor was protected by an elaborate system of land and sea walls, which included round towers (Hadjidaki, 1996; Hadjidaki, 2015; Pirazzoli et al., 1992). The second example of a rock-cut channel can be found in Leachion, which was the western harbor of ancient Corinth, likely built in the early 6th century BCE and remained in use until 400 AD. This was an artificial harbor with navigation channels that connected it to the sea (Morhange et al., 2012; Stiros et al., 1996). A well-fortified closed harbor with sea walls and round towers was found at

Thasos, the towers added to the sea wall at the end of the 4th century BCE (Empereur & Simossi, 1992; Lianos, 1993; Simossi, 1994–1995). It is possible that the idea to create fortified ports equipped with towers reached the coasts of the eastern Mediterranean during the Hellenistic period, as seen by the appearance of round towers in the port of Straton's Tower, the town preceding Caesarea (Raban, 1992). Dor should be seen as belonging to the tradition of the formalized creation of a harbor basin utilizing artificial features, which became more common in the Levant during the Hellenistic period (Yasur-Landau et al., 2018).

The South Bay is open from the west. However, as stated above, at the time of use as an anchorage, this approach would have been tricky due to the shallow-exposed reef at its entrance. The easier approach considering the prevalent wind, that is, the Dor channel was wide yet narrow enough that it could have been controlled from the adjacent towers. It is possible that it could have also been blocked by a chain to prevent unauthorized entry into the bay from the south, similar to that reported for Akko (from the Early Islamic period; Galili et al., 2010), or to the chain blocking at least one of the entrances to the harbor in Alexandria (Belov, 2014). While these harbors are dated to later periods than the South Bay, it could be feasible that such harbor protection existed this early on.

The abandonment of the South Bay harbor following the Byzantine period most likely came from over sedimentation, mixed with rising sea levels (Benjamin et al., 2017; Sivan et al., 2001). Josephus (2014), writing in the 1st century CE (*Antiquities of the Jews* 15:33) mentions Dor as a poor harbor, where winds and sand would impede landing operations and force merchants to anchor offshore (Kingsley & Raveh, 1994). Josephus (2014) wrote during the Roman Period and might have been referring to Dor's harbor before it was moved to the North Bay. Archaeological findings from the South Bay are dated at the latest to the Roman Period, while the main groups of artifacts in the North Bay began to appear during the Roman Period. Thus, this would be the most likely time for the transition between the two bays (ArkinShalev et al., 2019b).

The combination of land geophysics and marine archaeology presented in this study revealed anthropogenic intervention on the environment that has been buried in the sand due to sea-level rise and resulting sedimentation. Marriner et al. (2014) used geosarchaeological data to argue that the creation of artificial harbors in the southern Levant was a gradual process, moving from anchoring in bays and lagoons in the Bronze Age to partially modified bays during the Iron Age to fully artificial harbor basins in the Roman period. The new findings from Dor, using a combination of direct archaeological excavation and geophysical prospection, provide crucial evidence suggesting that the modification of natural anchorages was by itself a gradual process of elaboration: from the Tel-side mole and wall of the Iron Age to the combining of the Tantara Lagoon and South Bay into a unified anchoring system during the Hellenistic period. Anchoring was practiced both in the South Bay with its restricted access, yet also in the Tantara Lagoon leading into it, which also contains artifacts from the Iron Age, Hellenistic and Roman, and Byzantine Periods (ArkinShalev et al., 2019a; Kingsley & Raveh, 1996). Planned future archaeological excavations and coring in the area of the submerged structures and the channel uncovered here will no doubt present a

clearer plan of the structures as well as the depth and details of construction of the channel. This could have important implications for how the natural environment was first used for man's benefit but later had to be abandoned or modified as natural environmental processes became more dominant. Since sea-level rise is a problem that we are currently dealing with today, this study may help understand how it can affect modern-day harbors and anchorages in general, and not just in the eastern Mediterranean.

ACKNOWLEDGMENTS

This study was supported in part by the Israel Science Foundation Grant No. 495/18: An Underwater Study of Tel Dor Anchorages and Harbor Infrastructure. Additional funding was provided by the Koret Foundation as part of the UC San Diego SCMA Koret Israel Bridge-Building Program, the Norma Kershaw Endowed Chair in the Archaeology of Ancient Israel and Neighboring Lands, and the Phokion and Liz Anne Potamianos Family Foundation. The authors wish to thank the excavation team: Brigid Clark and Sara Lantos (Excavation Directors); Ariel Polakoff (Registrar); Anthony Tamborino (Digital Recording); Amir Yurman, Moshe Bachar, and Rich Walsh (Dive Safety Officers); Aviva Pollack (Underwater Plans); Lilach Meyer (Administrator). Thank you to the anonymous reviewers for their time in improving the manuscript.

DATA AVAILABILITY STATEMENT

The data that support the findings of this study are available from the corresponding author upon reasonable request.

AUTHOR CONTRIBUTIONS

Michael Lazar conceived, formally analyzed, investigated, methodized, supervised, validated, visualized, wrote the original draft, reviewed, and edited the manuscript. Uri Basson curated the data, formally analyzed, methodized, helped with software, visualized, wrote the original draft, reviewed, and edited the manuscript. Ashley G. Himmelstein formally analyzed, investigated, and visualized. Thomas E. Levy acquired the funding, investigated, and resources. Ehud Arkin Shalev helped with investigation and validation. Assaf Yasur-Landau conceptualized, acquired the funding, helped with investigation and resources, methodized, wrote the original draft, reviewed, and edited the manuscript.

ORCID

Michael Lazar  <http://orcid.org/0000-0003-0892-5166>

REFERENCES

- Arkin Shalev, E., Gambash, G., & Yasur-Landau, A. (2019a). Disheveled Tenacity: The North Bay of Roman and Byzantine Dor. *Journal of Maritime Archaeology*, 14, 205–237.
- Arkin Shalev, E., Gilboa, A., & Yasur-Landau, A. (2019b). The Iron Age Maritime Interface at the South Bay of Tel Dor: results from the 2016 and 2017 excavation seasons. *International Journal of Nautical Archaeology*, 48, 439–452.
- Basson, U., Ben-Avraham, Z., Garfunkel, Z., & Lyakhovsky, V. (2002). Development of recent faulting in the southern Dead Sea Rift according to GPR imaging. *European Geophysical Society (EGS) Stephan Mueller Special Publication Series*, 2, 1–23.
- Basson, U., & Ginzburg, A. (2009). *Mapping Archaeological Remains at the Baniyas using ground penetrating radar (GPR)*. Baniyas IAA Report, Paneas II: Finds and Other Studies.
- Beck, A., & Kravtsov, A. (1998). *Geophysical survey using seismic refraction for subsurface mapping in the coast of Dor* (Report 217/65/97). The Geophysical Institute of Israel, pp. 5 (In Hebrew).
- Belov, A. (2014). *Navigational aspects of calling to the Great Harbour of Alexandria*. Halshs-00845524f. Retrieved from https://halshs.archives-ouvertes.fr/halshs-00845524/file/Belov.A_forthcoming_Navigational_aspects_of_calling_to_the_Great_Harbour_of_Alexandria.pdf
- Benjamin, J., Rovere, A., Fontana, A., Furlani, S., Vacchi, M., Inglis, R. H., Galili, E., Antonioli, F., Sivan, D., Miko, S., Mourtzas, N., Felja, I., Meredith Williams, M., Goodman-Tchernov, B., Kolaiti, E., Anzidei, M., & Gehrels, R. (2017). Late Quaternary sea-level changes and early human societies in the central and eastern Mediterranean Basin: An interdisciplinary review. *Quaternary International*, 449, 29–57.
- Best, M. E. (2015). Electromagnetic (EM) methods. In (Eds.) Hunter, J. A. & Crow, H. L., *Shear wave velocity measurement guidelines for Canadian seismic site characterization in soil and rock* (pp. 170–180). Geological Survey of Canada, Earth Science Sector, General Information Product.
- Bourbie, T., Coussy, O., & Zinszner, B. (1987). *Acoustics of porous media*. Gulf Publishing Company.
- Bristow, C. S. & Jol, H. M., (Eds.). (2003). *Ground penetrating radar in sediments*. Geological Society of London.
- Cohen-Seffer, R., Greenbaum, N., Sivan, D., Barneir, E., Croitoru, S., & Inbar, M. (2005). Late Pleistocene–Holocene marsh episodes along the Carmel coast, Israel. *Quaternary International*, 140–141, 103–120.
- Conyers, L. B. (2004). *Ground-penetrating radar for archaeology*. AltaMira Press.
- Empereur, J. Y., & Simossi, A. (1992). Travaux de l'école française en Grèce en 1991. Thasos. Le port. *Bulletin de Correspondance Hellénique*, 116, 721–726.
- Galili, E., Rosen, B., Zviely, D., Silberstein, N. A., & Finkielsztejn, G. (2010). The evolution of Akko harbor and its Mediterranean maritime trade links. *Journal of Island and Coastal Archaeology*, 5, 191–211.
- Gilboa, A. (2015). Dor and Egypt in the Early Iron Age: An archaeological perspective of (Part of) the Wenamun report. *Egypt and the Levant*, 25, 247–274.
- Gilboa, A., & Sharon, I. (2008). Between the Carmel and the sea: Tel Dor's Iron Age reconsidered. *Near Eastern Archaeology*, 71, 146–170.
- Goldshleger, N., & Basson, U. (2016). Utilization of ground-penetrating radar and frequency domain electromagnetic for investigation of sewage leaks. *Environmental Applications of Remote Sensing*, Chapter 9, 261–280.
- Goldshleger, N., Basson, U., Fastig, S., & Azaria, I. (2018). Using combined close-range active and passive-remote sensing methods to detect sinkholes. *Journal of Remote Sensing and GIS*, 7, 222.
- Goldshleger, N., Shamir, O., Basson, U., & Zaadi, E. (2019). Frequency domain electromagnetic method (FDEM) as a tool to study contamination at the sub-soil layer. *Geosciences*, 9, 382.
- Goldsmith, V., Rosen, P., & Gertner, Y. (1990). Chapter Five – Eolian transport measurements, winds, and comparison with theoretical transport in Israeli coastal dunes. In (Eds.) Nordstrom, K. F., Psuty, N. P. & Carter, R. W. G., *Coastal Dunes: Form and Process* (pp. 79–101). London: John Wiley & Sons Ltd.
- Hadjidaki, E. (1996). The Hellenistic Harbour of Phalasarna in Western Crete: A comparison with the Hellenistic Inner Harbour of Straton's Tower. In (Eds.) Raban, A. & Holum, K. G., *Caesarea Maritima: Retrospective after two Millennia* (pp. 53–64). Netherlands: Brill.
- Hadjidaki, E. (2015). Recent finds from the harbor of ancient Phalasarna. In (Eds.) Karanastasi, P., Tsigounaki, A. & Tsigonaki, C., *Archaeological work on Crete volume 2 3* (pp. 127–134). Rethymon.
- Haggi, A., & Artzy, M. (2007). The Harbor of Atlit in Northern Canaanite/Phoenician context. *Near Eastern Archaeology*, 70, 75–84.

- Huang, H. (2005). Depth investigation for small broadband electromagnetic sensors. *Geophysics*, 70, 135–142.
- Huang, H., & Won, I. J. (2003). Real-time resistivity sounding using a handheld broadband electromagnetic sensor. *Geophysics*, 68, 1224–1231.
- Josephus, F. (2014). Judean Antiquities 15. In Jan Willem Henten (Ed.), *FJTC 7b*. Leiden: Brill. van.
- Kadosh, D., Sivan, D., & Kutiel, H. (2004). A late quaternary paleoenvironmental sequence from Dor, Carmel coastal plain, Israel. *Palynology*, 28, 143–157.
- Kahanov, Y. (2011). Ship reconstruction, documentation, and in situ recording. In (Eds.) Catsambis, A., Ford, B. & Hamilton, L. D., *The Oxford Handbook of Maritime Archaeology* (pp. 161–181). New York: Oxford University Press.
- Kingsley, S. A., & Raveh, K. (1994). A reassessment of the northern harbour of Dor, Israel. *International Journal of Nautical Archaeology*, 23, 289–295.
- Kingsley, S. A., & Raveh, K. (1996). *The ancient harbour and anchorage at Dor, Israel: Result of the underwater surveys 1976–1991*. Oxford: Tempus Reparatum.
- Lazar, M., Engoltz, K., Basson, U., & Yasur-Landau, A. (2018). Water saturated sand and a shallow bay: combining coastal geophysics and underwater archaeology in the south bay of Tel Dor. *Quaternary International*, 473, 112–119.
- Lianos, N. A. (1993). *The area of the ancient closed of Thasos (A preliminary report)*. Tropis V: 133–160.
- Marriner, N., Morhange, C., Kaniewski, D., & Carayon, N. (2014). Ancient Harbour Infrastructure in the Levant: Tracking the Birth and Rise of New Forms of Anthropogenic Pressure. *Scientific Reports*, 4, 1–11.
- Morhange, C., Pirazzoli, P. A., Evelpidou, N., & Marriner, N. (2012). Late Holocene tectonic uplift and the silting up of Lechaion, the western harbor of ancient Corinth, Greece. *Geoarchaeology*, 27, 278–283.
- Nitschke, J. L., Martin, S. R., & Shalev, Y. (2011). Between Carmel and the sea: Tel Dor: The Late Periods. *Near Eastern Archaeology*, 74, 132–154.
- Pirazzoli, P. A., Ausseil-Badie, J., Giresse, P., Hadjidaki, E., & Arnold, M. (1992). Historical environmental changes at Phalasarna harbor. *West Crete. Geoarchaeology*, 7, 371–392.
- Raban, A. (1992) In search of Straton's tower. In R. Vann (Ed.), *Caesarea papers: Straton's tower, Herod's harbour, and Roman and Byzantine Caesarea* (pp. 7–22). *Journal of Roman Archaeology, Supplementary Series 5*.
- Raban, A. (1995). Dor-Yam: Maritime and coastal installations at Dor in their geomorphological and stratigraphic context. In (Ed.) Stern, E., *Areas A And C: Introduction and Stratigraphy. Vol. 1A of Excavations at Dor, Final Report. Qedem Reports 1* (pp. 286–354). Jerusalem: Institute of Archaeology and The Hebrew University of Jerusalem In Cooperation with The Israel Exploration Society.
- Rogers, M., Leon, J. F., Fisher, K. D., Manning, S. W., & Sewell, D. (2012). Comparing similar ground-penetrating radar surveys under different moisture conditions at Kalavassos-Ayios Dhimitrios, Cyprus. *Archaeological Prospection*, 19, 297–305. <https://doi.org/10.1002/arp.1435>
- Saaroni, H., Ziv, B., Bitan, A., & Alpert, P. (1998). Easterly Wind Storms over Israel. *Theoretical and Applied Climatology*, 59, 61–77.
- Sharon, I. (1995). The Stratigraphy of areas A and C. In (Ed.) Stern, E., *Areas A and C: Introduction and stratigraphy. Vol. 1A of excavations at Dor, final report* (pp. 49–234). Jerusalem: Qedem Reports 1. Institute of Archaeology and The Hebrew University of Jerusalem In Cooperation with The Israel Exploration Society.
- Sharvit, J., Baxton, B., & Planer, D. (2013). Preliminary findings from archaeological excavations along the foot of the southern Seawall at Akko, 2008–2012. *Michmanim*, 24, 39–52.
- Simossi, A. (1994–1995). To archaio polemiko limani tes Thasou. *Archaologikon Deltion* 49–50. *Meletes A*.
- Sivan, D., Eliyahu, D., & Raban, A. (2004). Late Pleistocene to Holocene wetlands now covered by sand, along the Carmel Coast, Israel, and their relation to human settlement: an example from Dor. *Journal of Coastal Research*, 204, 1035–1048.
- Sivan, D., Wdowinski, S., Lambeck, K., Galili, E., & Raban, A. (2001). Holocene sea-level changes along the Mediterranean Coast of Israel, based on archaeological observations and numerical model. *Palaeogeography, Palaeoclimatology, Palaeoecology*, 167, 101–117.
- Spies, B. R. (1989). Depth of investigation in electromagnetic sounding methods. *Geophysics*, 54, 872–888.
- Stern, E. (1994). *Dor ruler of the seas*. Biblical Archaeology Society.
- Stiros, S., Pirazzoli, P., Rothaus, R., Papageorgiou, S., Laborel, J., & Arnold, M. (1996). On the date of construction of Lechaion, western harbor of ancient Corinth, Greece. *Geoarchaeology*, 11, 251–263.
- Sudduth, K. A., Kitchen, N. R., Wiebold, W. J., Batchelor, W. D., Bollero, G. A., Bullock, D. G., Clay, D. E., Palm, H. L., Pierce, F. J., Schiler, R. T., & Thelen, K. D. (2005). Relating apparent electrical conductivity to soil properties across the northcentral USA. *Computers and Electronics in Agriculture*, 46, 263–283.
- Swarzenski, P. W., Burnett, W. C., Greenwood, W. J., Herut, B., Peterson, R., Dimova, N., & Weinstein, Y. (2006). Combined time-series resistivity and geochemical tracer techniques to examine submarine groundwater discharge at Dor Beach, Israel. *Geophysical Research Letters*, 33, 1–6.
- Todd, D. K., & Mays, L. W. (2004). *Groundwater Hydrology* (3rd ed.). Wiley Publishing.
- Won, I. J., Keiswetter, D. A., Fields, G. R. A., & Sutton, L. C. (1996). GEM-2: A new multifrequency electromagnetic sensor. *Journal of Environmental and Engineering Geophysics*, 1, 89–157.
- Yasur-Landau, A. (2019). The Memory Machine: How 12th BCE century Iconography Created Memories of the Philistines (and other Sea Peoples). In E. Borgna, R. Laffineur, I. Caloi, & F. M. Carinci (Eds.), *Past and Memory in the Aegean Bronze Age* (pp. 413–422). Proceedings of the 17th International Aegean Conference, University of Udine, Department of Humanities and Cultural Heritage, Ca' Foscari University of Venice, Department of Humanities, 17–21 April 2018 (Aegaeum 43). Liège.
- Yasur-Landau, A., Arkin Shalev, E., Zajak, P. R., & Gambash, G. (2018). Rethinking the Anchorages and Harbours of the Southern Levant 2000 BC–600 AD. In C. von Carnap-Bornheim, F. Daim., P. Ettel, & U. Warnke (Eds.), *Harbours as objects of interdisciplinary research* (pp. 73–89). Proceedings of the International Conference Harbours as objects of interdisciplinary research – Archaeology+History +Geosciences, Christian-Albrechts-University, Kiel.
- Zviely, D., Kit, E., & Klein, M. (2007). Longshore sand transport estimates along the Mediterranean coast of Israel in the Holocene. *Marine Geology*, 238, 61–73.

How to cite this article: Lazar M, Basson U, Himmelstein AG, Levy TE, Arkin Shalev E, Yasur-Landau A. The door to Dor: Tracing unseen anthropogenic impact in an ancient port. *Geoarchaeology*. 2020;1–10. <https://doi.org/10.1002/gea.21825>